**EPJ manuscript No.**
(will be inserted by the editor)

# Nuclear Thermometry

Aleksandra Kelić[1], Joseph B. Natowitz[2] and Karl-Heinz Schmidt[1]

[1] GSI, Planckstr. 1, 64291 Darmstadt, Germany
[2] Department of Chemistry, Texas A&M University, College Station, TX 77842, USA

Received: date / Revised version: date

**Abstract.** Different approaches for measuring nuclear temperatures are described. The quantitative results of different thermometer approaches are often not consistent. These differences are traced back to the different basic assumptions of the applied methods. Moreover, an overview of recent theoretical investigations is given, which study the quantitative influence of dynamical aspects of the nuclear-reaction process on the extracted apparent temperatures. The status of the present experimental and theoretical knowledge is reviewed. Guidelines for future investigations, especially concerning the properties of asymmetric nuclear matter are given.

**PACS.** 24.60.-k Statistical theory and fluctuations in nuclei – 05.70.Fh Phase transitions: general studies – 25.70.-z Low and intermediate energy heavy-ion reactions – 21.10.Ma Nuclear level density

## 1 Introduction

The concept of a nuclear temperature was introduced some seventy years ago in pioneering works performed by Bethe [1] and Weisskopf [2]. The goal was to describe the formation and the decay of a compound nucleus formed in reactions induced by light projectiles, mostly neutrons. Later on, the concept of a nuclear temperature was extended to reactions involving high-energy projectiles and heavy ions [3]. These new studies were triggered by the quest for nuclear instabilities and a possible liquid-gas phase transition in nuclear matter [4,5]. To this goal, different experimental methods were developed and applied in order to extract information on thermal characteristics of highly excited nuclear systems (see e.g. [6] and references therein). Most of these "nuclear thermometers" rely on the application of thermodynamic relations to characterize the conditions at freeze-out. In general, the temperature of a system with fixed number of particles $N_{part}$ at an energy $E$ is defined according to the statistical mechanics as:

$$\frac{1}{T} = \frac{\partial S(E, N_{part})}{\partial E} = \frac{\partial \ln \rho(E, N_{part})}{\partial E} \qquad (1)$$

where, $S$ is the entropy of the system, and $\rho$ the density of states at energy $E$. In order to apply this formula to obtain a temperature, two conditions have to be fulfilled: Firstly, the system has to be in full statistical equilibrium, i.e. each of the states included in $\rho(E, N_{part})$ has to be populated with equal probability, and secondly the density of states has to be known. For nuclear systems these two conditions can be critical. The degree to which the equilibrium is reached in high-energy heavy-ion collisions is not a priori known as the dynamical evolution of a nuclear system is still not fully understood. What concerns the nuclear state density, it is well known only at low energies. At high excitation energies, on the contrary, the knowledge of the nuclear state density is much poorer.

Apart from this, there are several other problems, which make the extraction of nuclear temperatures even more difficult:

- *The nucleus is a microscopic system* - External probes are not applicable. Consequently, information on temperature is obtained from the emission of (small) parts of the system itself assuming that the emitted clusters made part of the equilibrium and the density of states of the whole system before emission, and are, therefore, representative for the whole system.

- *The nucleus is an isolated system* - Due to the short range of the nuclear force, the nucleus cannot exchange its excitation energy with its external environment. Consequently, the nuclear system is defined by the conditions: $E = const$, $N_{part} = const$, and, therefore, the only appropriate statistical ensemble in case of the nucleus is the microcanonical ensemble used for isolated systems [6,7]. On the other hand, from the experiment it is not that easy to fix the value of energy, as the amount of deposited energy can vary strongly between different nuclear collisions, especially in cases where several different reaction mechanisms result in the emission of the same product.

- *The nucleus is a quantum Fermionic system* - Nucleons inside the nucleus occupy different energy levels, and, moreover, due to the Pauli principle not all nucleons can participate in sharing the available energy. Consequently, the effective number of degrees of freedom depends on excitation energy, what is accounted for by the Fermi statistics. Moreover, the global properties of a nucleus change

dynamically with energy (e.g. the density of the nucleus reduces due to thermal expansion).

- *The nucleus is an electrically charged system* - The long-range Coulomb force between protons introduces instabilities [8] that could lead to a lowering of the critical temperature.

- *The nucleus heats up and cools down in a dynamical process* - Different signatures may correspond to different freeze-out conditions, or represent different stages in the dynamical evolution. Moreover, production during evaporation can contribute to the yields of light fragments, while expansion influences the kinetic energy of the fragments.

- *The thermodynamical parameters (e.g. pressure, volume, chemical potential) are not under control* - In the experiment one does not have direct access to thermodynamical parameters and is obliged to use model calculation in order to extract them.

- *Experimental signatures are modified by secondary decay* - Consequently, in most cases one needs robust signatures, which are least affected by secondary decay (e.g. light IMFs).

## 2 Thermometer methods

In the literature, different thermometer methods have been applied. According to their approach they can be grouped as:

- *Population approaches* - Based on the grandcanonical concept. The value of the nuclear temperature is extracted from the yields of the produced clusters assuming a Boltzmann distribution: $Y_i \sim exp(-E_i/T)$. The most often used methods are: Double ratios of isotopic yields [9,10], also called isotopic thermometer; Population of excited states (bound or unbound) [6,11–16]; Isobaric yields from a given source [17,18].

- *Kinetic approaches* - Based on the concept of a canonical ensemble. The value of the temperature is extracted from the slope of the measured particle kinetic-energy spectra; due to this, the method is named slope thermometer. Two processes are studied within this approach: Thermal evaporation from the compound nucleus [2] and sudden disintegration of an equilibrated source into observed nucleons and light nuclei [19–23] or gamma rays [24,25].

- *Thermal-energy approaches* - The excitation energy at the freeze-out is extracted by measuring the evaporation cascade from a thermalised source by variation of neutron-to-proton ratio *N/Z*. The temperature at freeze-out is then obtained from the deduced excitation energy. An example is the isospin thermometer [26,27].

### 2.1 Population Approaches

#### 2.1.1 Double Ratios of Isotopic Yields

This method evaluates the temperature of equilibrated nuclear regions from which light fragments are emitted using the yields of different light nuclides [9]. The basic assumptions of the method are those of the grandcanonical approach.

During the cooling and expansion stage of a hot nuclear system, the interactions between the constituent particles take place until density and temperature become small enough so that the constituents do not longer interact. From this time on the particle composition remains unchanged (chemical freeze-out). As the system expands beyond this point the frozen particles escape. By detecting them one can obtain information on the freeze-out stage. The starting assumption of the method is that thermal equilibrium is established between free nucleons and composite fragments contained within a certain interaction volume $V$ at a temperature $T$. In this case, the density of a particle $(A,Z)$ is [9]:

$$\rho(A,Z) = \frac{N_{part}}{V} = \frac{A^{3/2}\cdot\omega(A,Z)}{\lambda^3}\cdot\exp(\frac{\mu(A,Z)}{T}) \quad (2)$$

where $\omega$ is the internal partition function of the particle $(A,Z)$: $\omega(A,Z) = \sum[2\cdot s_j(A,Z)+1]\cdot\exp[-E_j(A,Z)/T]$, $\lambda$ is the thermal nucleon wave-length $\lambda = h/\sqrt{2\cdot\pi m_N\cdot T}$, and $\mu$ is the chemical potential of the particle $(A,Z)$.

In the next step, one imposes to the system also the condition of chemical equilibrium: $\mu(A,Z) = Z\cdot\mu_{pF} + (A-Z)\cdot\mu_{nF} + B(A,Z)$, $B$ being the binding energy of the cluster $(A,Z)$, and $\mu_{pF}$ and $\mu_{nF}$ the chemical potentials of free protons and neutrons, respectively.

Then for the ratio $Y(A,Z)/Y(A',Z')$ between the measured yields of two different emitted fragments one gets [9]:

$$\frac{Y(A,Z)}{Y(A',Z')} = \frac{\rho(A,Z)}{\rho(A',Z')} = (\frac{A}{A'})^{3/2}\cdot(\frac{\lambda^3}{2})^{A-A'}\cdot \frac{\omega(A,Z)}{\omega(A',Z')}\cdot\rho_{pF}^{Z-Z'}\rho_{nF}^{(A-Z)-(A'-Z')}\cdot \exp(\frac{B(A,Z)-B(A',Z')}{T}) \quad (3)$$

with $\rho_{pF}$ and $\rho_{nF}$ being, respectively, the densities of free protons and neutrons contained in the same interaction volume $V$ at the temperature $T$ as the cluster $(A,Z)$. Using Eq. 3 and two sets of the yields of two fragments differing only by one proton one obtains the temperature of the emitting source at the moment of freeze-out [9]:

$$T = (\Delta B_1 - \Delta B_2)/\ln[(\frac{Y(A_1,Z_1)/Y(A_1+1,Z_1+1)}{Y(A_2,Z_2)/Y(A_2+1,Z_2+1)}) \cdot(\frac{(A_1+1)\cdot A_2}{A_1\cdot(A_2+1)})^{3/2}\cdot(\frac{\omega(A_1+1,Z_1+1)\cdot\omega(A_2,Z_2)}{\omega(A_1,Z_1)\cdot\omega(A_2+1,Z_2+1)})] \quad (4)$$

where, $\Delta B_i = B(A_i,Z_i) - B(A_i+1,Z_i+1)$, $i$=1,2. An analogous relation is obtained if one takes pairs of nuclei differing only by one neutron.

When applying this method to extract the value of the nuclear temperature, several precautions have to be made. Firstly, as this method assumes that both thermal and chemical equilibrium at the freeze-out are reached, it

is important to consider only those yields which can be attributed to the equilibrium component of the whole reaction mechanism. Secondly, one has to be sure that the studied light particles are emitted during the freeze-out and not as the product of secondary decay [28–30]. Moreover, the side-feeding to the considered nuclides from secondary decay can also result in a large spread of extracted temperature values. Finally, in order to obtain the value of nuclear temperature one needs to calculate the binding energies of observed fragments, see Eq. 4. Although Eq. 4 describes the situation at the freeze-out very often in its application the experimental binding energies have been used. One should not forget that a binding energy depends on the symmetry-energy coefficient used in the mass formula, which might depend on density and temperature, and, therefore, the use of experimental binding energies in order to describe the situation at the freeze-out could be questionable.

#### 2.1.2 Population of Excited States

This method has the same basic assumptions as the double-isotopic-ratio method. The departure point is that the population distribution of the excited states in a statistically equilibrated system should be given by the temperature of the system and by the spacing between the considered energy levels. The advantage of this method as compared to the double-isotopic-ratio method is that one can assume that isospin and dynamical aspects influencing the population of the two considered states are the same.

Following this picture, the ratio $R$ of the populations of two states (if no feeding by particle decay takes place) is given, similar to Eq. 3, as:

$$R = \frac{2 \cdot j_u + 1}{2 \cdot j_l + 1} \cdot \exp(-\frac{\Delta E}{T}) \qquad (5)$$

where, $j_u$ and $j_l$ are the spins of the upper and lower state, respectively, and $\Delta E$ the energy difference between these two states. This energy difference limits the temperature that can be inferred by this method, as for temperatures higher than $\Delta E$ one reaches saturation, i.e. the ratio $R$ approaches its asymptotic high-temperature value. The considered excited states can be either particle-bound or particle-unbound states. The advantage of taking particle-unbound states lies in the fact that for the unbound states $\Delta E$ has, generally, higher values than for the bound states, thus, allowing for the measurement of higher temperatures. Moreover, the relative population between ground state and particle-bound state can be changed by the sequential decay of primary fragments produced in a particle-unbound state [11] or by the hadronic final-state interactions that occurs after emission from the equilibrated system [31]. This is important, as in cases where the primary population ratio is strongly influenced by secondary decays the uncertainties in the extracted temperature can be large [11].

#### 2.1.3 Isobaric Yields from a Given Source

This thermometer is mostly applied in studies of the thermal properties of excited quasiprojectiles formed in heavy-ion reactions in the Fermi energy regime. It uses the model assumptions of the statistical multifragmentation model [5], according to which, in the grandcanonical picture, the ratio between yields of two observed fragments having the same ground-state spins and coming from the same source is given as [17]:

$$\frac{Y(A_1, Z_1)}{Y(A_2, Z_2)} = \exp[-\frac{1}{T} \cdot (F_{A1,Z1}(T, V) - F_{A2,Z2}(T, V) - \mu_n \cdot (N_1 - N_2) - \mu_p \cdot (Z_1 - Z_2))] \qquad (6)$$

with $F(T,V)$ the internal free energy of the fragment, $N_i = A_i - Z_i$, $T$ and $V$ freeze-out temperature and volume, respectively. The internal free energy is calculated as given in [5]. The results of this thermometer using the $Y(^3\mathrm{H})/Y(^3\mathrm{He})$ ratio compares very well with results of double-isotopic-ratio methods using $^2$H,$^3$ H/$^3$He,$^4$ He ratios [17]. The problems inherent to the previous two methods are also present in the isobaric-yields method.

### 2.2 Kinetic Approaches

The method of the slope thermometer is based on fitting the exponential slope of measured particle spectra. The spectral distributions of particles emitted by an excited nucleus were firstly described by Weisskopf in case of neutron-induced reactions using the standard thermodynamic procedure [2]. The predicted spectra followed a Maxwell-Boltzmann distribution proportional to an energy-dependent pre-exponential factor and the Boltzmann function: $dY/dE_{kin} = f(E_{kin}) \exp(-E_{kin}/T)$. The shape of the particle spectra was later discussed by Goldhaber who mostly concentrated on the form of the pre-exponential factor [32].

This method is applied to two processes:

- *Thermal evaporation form the compound nucleus* - Except at very low excitation energies, the decay of an excited nucleus proceeds through several deexcitation steps. Consequently, the mass and the temperature of the emitting source vary in time, and the observed spectra represent the convolution of all these different contributions. Therefore, for fitting the measured spectra dedicated models that properly describe the time evolution of the cooling process have to be applied (e.g. [33–38]).

- *Sudden disintegration* - One assumes a single freeze-out configuration from which nucleons and light particles are emitted. In this case, dynamical effects to be mentioned below if not properly described can lead to misleading results concerning the magnitude of the extracted nuclear temperature. Additional difficulties arise from the fact that the observed fragment can emerge from any location in the source, and that its Coulomb energy depends on the number and position of all the other created fragments [39]. Moreover, the Fermi motion of nucleons inside

the projectile/target as well as inside the source has to be considered. The nucleonic Fermi motion within the colliding nuclei has been discussed by Goldhaber as origin of the momenta of the produced fragments in fragmentation reactions [40]. He has also pointed out that the resulting behavior, i.e. the form of the fragment kinetic energies, is indistinguishable from that of a thermalised system with rather high temperature. Its relevance for the interpretation of the kinetic properties of nuclear decay products has been underlined by Westfall et al. [21]. In ref. [22], it was discussed that the slope temperature does not correspond to the thermal temperature at the freeze-out but rather reflects the intrinsic Fermi motion and, thus, the bulk density of the spectator system at the moment of break-up. This would suggest that it may be difficult to attribute the slope parameter of the energy spectra of the observed light fragments directly to the thermal characteristics of the decaying system. As in the case of surface emission, the temporal evolution of the emitting source [33,41,42] as well as the sequential decay of excited primary fragments [33,43] can complicate the interpretation of the measured kinetic-energy spectra. Recently, it was proposed to use the energy spectra of thermal Bremsstrahlung photons in order to extract the nuclear temperature at the freeze-out [24,25]. The advantage of using gamma rays instead of nucleons and light particles should lay in the following facts: minimal contribution from pre-equilibrium processes, absence of the reacceleration by the Coulomb field, sensitivity on the temperature of the system right after equilibration, and absence of final-state distortions [24].

The shape of the measured particle spectra can be influenced by collective dynamical effects - collective rotation [44,45], translatory motion [20,41] and collective expansion of the source [46,47]. Each of these effects can influence the spectra in a similar way as the changes in the temperature; for more details see ref. [6].

### 2.3 Thermal Approaches

Thermal approaches are based on the assumption that the thermal energy after the freeze-out feeds an evaporation cascade. The excitation energy at the freeze-out is extracted by measuring the evaporation cascade from a thermalised source by detecting either final residues [26, 27] or light charged particles [48,49]. While for the other methods, the secondary decay is a disturbing effect, in thermal approaches the evaporation cascade is used to deduce the temperature at the freeze-out, and it is, therefore, also applicable to heavy reaction residues.

In the first approach - isospin thermometer - one gains information on the excitation energy and, consequently, on the temperature at the freeze-out configuration by backtracing the evaporation cascade [27]. This idea is the base of the "thermometer for peripheral nuclear collisions" [26], a method to deduce the temperature of nuclear systems from the isotopic distributions of the residues at the end of the evaporation cascade. The method consists of applying an evaporation code with the quite well known ingredients of the statistical model in order to deduce the temperature at the beginning of the evaporation cascade. In this approach, the mean neutron-to-proton ratio of the final residues is calculated for different freeze-out temperatures, assuming that the $N/Z$ ratio of fragments at the freeze-out is the same as that of the projectile. By obtaining agreement between measured and calculated $N/Z$ ratios one deduces the value of nuclear temperature at the freeze-out. The assumption that the fragments enter the evaporation stage with the same $N/Z$ as the projectile or respectively target nucleus is rather simplifying, since according to some descriptions of the nuclear break-up (e.g. [50,51]), the process of isospin fractionation should result in different isotopic compositions in case of heavy and light fragments (i.e. liquid and gas phase), leading to a more neutron-rich gas phase and a less neutron-rich liquid phase. While neglecting the isospin-fractionation process will likely introduce only a small uncertainty, details of the evaporation model especially at high excitation energy are important for the qualitative application of the isospin thermometer [52]. The isospin thermometer is mostly applied at relativistic energies as at Fermi energies the effect of isospin diffusion [53] can complicate the interpretation of this method.

In the second case [48,49], a correlation technique for the relative velocity between light charged particles and IMF is applied in order to extract multiplicities and velocity spectra of secondary evaporated particles. From this information the average size and average excitation energy of the primary hot fragments is reconstructed.

## 3 Corrections

One should not forget that one of the reasons for measuring the nuclear temperature is the possibility to reconstruct the nuclear caloric curve and to search for possible evidence of a liquid-gas phase transition. Very often, the predictions of different thermometers differ dramatically (see e.g. [54]), and it is, therefore, of prime interest to understand and apply all possible corrections that can influence the value of the obtained nuclear temperature.

Before we start the more detailed discussion on different corrections to be applied, we would like to express a word of caution - most methods mentioned above cannot result in the "correct" thermodynamical temperature of the nucleus, as they are all based either on the canonical or grandcanonical ensemble, but not on the microcanonical ensemble. Moreover, due to the basic difference between different methods (e.g. canonical versus grandcanonical approach) one should not expect that the obtained, apparent, temperatures have the same values. One should also not forget that the measured quantity might reflect the temperatures on different stages (times) or different regions (positions) of the system, and this is also one of the reasons for different values of the apparent temperature. In connection with this, one can also pose the question if some of the basic assumptions of different methods, i.e. establishment of thermal and/or chemical equilibrium, are fulfilled in nuclear reactions. And if so, are the measured observables characteristic of the established equilibrium?

An optimistic answer was given in ref. [55], where it was shown that caloric curves obtained using the above mentioned thermometer methods can still carry the signal of the phase transition in a system with conserved energy.

If one assumes the validity of different thermometer methods, in order that they are applicable one has first to consider several corrections, and here we will discuss some of them: finite-size effects [39,56], emission-time differences [57], multi-source emission [58], secondary decay [28–30,59] and recombination [60].

### 3.1 Finite-Size Effects

One of the consequences of applying the canonical or grand-canonical ensemble is that effects due to the finite size of the nucleus are neglected. In ref. [56] caloric curves obtained using different double-isotopic-ratio thermometers were compared with the results of microcanonical calculations [4,61]. Results of this comparison have shown that there are important differences between different double-isotopic-ratio temperatures themselves, as well as between double-isotopic-ratio temperatures and microcanonical temperatures. These deviations are especially important at higher excitation energies above $\sim 8$ MeV/nucleon.

The authors of ref. [56] proposed a method, independent of the size of the source, to "calibrate" the different thermometers using the microcanonical temperature. They applied this procedure to re-evaluate different experimental caloric curves (ALADIN [10], EOS [62], INDRA [63]). The re-evaluated caloric curves show the features of a liquid-gas phase transition, which were missing in the original experimental data.

### 3.2 Emission-Time Differences

During a nuclear reaction, processes occurring on different time scales (e.g. fast break-up, pre-equilibrium emission, evaporation from the compound system) contribute to the production of the observed fragments and light particles. Fragments produced by these different mechanisms can have quite different characteristics (e.g. $N/Z$ ratio, velocity, angular distribution), and already Albergo et al. have discussed the importance of selecting a proper subset of observed events [9]. The influence of the reaction dynamics on the observed yields of different isotopic thermometers was studied in ref. [57] in more details. It was shown that the single ratios $Y(A,Z)/A(A+1,Z)$ involving one nuclide with $N < Z$ have several times higher values at forward angles as compared to the backward angles, while the single ratios including only $N \geq Z$ nuclides are approximately independent of the emission angle, the bombarding energy or the target-projectile system [57]. Based on the expanding-evaporating source model EES [47] these observations were interpreted as a consequence of differences in relative emission times of processes leading to the final fragments [57]. Similarly, Hudan et al. have found that in mid-peripheral and central collisions, isotopes with $N < Z$ have larger kinetic energies than heavier isotopes of the same element [58]. The same was observed by Liu et al. [64] for central collisions, and was explained by shorter emission times for neutron-deficient isotopes.

### 3.3 Multi-Source Emission

Production of light charged particles and intermediate-mass fragments is not only connected with different emission times, but also with different emitting sources. The composition and excitation energy of the emitting source can influence the size, composition and kinetic energy of the observed fragments [65,66], and, consequently, the value of the temperature extracted from yields or kinetic-energy spectra of fragments.

For example, it was shown in ref. [58] that fragments emitted from the mid-velocity source have broader peaks and higher tails in transverse-velocity distributions and are more neutron rich as compared to fragments emitted from the projectile-like source. In ref. [67] a detailed study on the validity, accuracy and experimental limits of the excitation energy measurements in the Fermi-energy regime has been performed. There, it was shown that difficulties in separating particles coming from different sources, especially for mid-peripheral and central collisions, as well as different experimental thresholds and cuts can lead to uncertainties in the source reconstruction.

Therefore, it is very important to identify in a experiment all different sources that contribute to the production of the observed fragments and their characteristics. Otherwise, the extracted value of the nuclear temperature will represent an average over different processes and conditions.

### 3.4 Recombination

In statistical models based on the canonical or grand-canonical ensemble, the momentum distribution of fragments is Maxwellian at the corresponding temperature, and, consequently, there is a probability that some pairs of primary fragments come close enough to feel the nuclear force and may recombine to form an excited heavier fragment, which may also decay later. This question on the evolution of the primary fragments under the combined influence of Coulomb and nuclear fields was studied in refs. [60,68]. Samaddar et al. have shown that, while the calculations without recombination predict an increase in the temperature with excitation energy similar to the Fermi-gas model predictions, inclusion of the recombination effect resulted in a decrease of the nuclear temperature and a plateau in the caloric curve [60].

On the other hand, in models based on the micro-canonical ensemble [4,61], the momenta and positions of the fragments are coupled, and the probability of having two fragments close in the freeze-out volume is strongly reduced by the Coulomb repulsion. Consequently, the effects of recombination may be reduced as compared to the above mentioned results. Therefore, it would be very

interesting to perform more detailed and dedicated calculations based on the microcanonical ensemble in order to quantitatively understand the recombination effect.

### 3.5 Secondary Decay

The primary fragments produced at the freeze-out stage are usually highly excited and they can undergo secondary decays. Such decay is evidenced, for example, in refs. [48, 49] in which a method based on correlations between light charged particles and IMF was applied in order to extract multiplicities and velocity spectra of particles emitted during the evaporation from the primary hot fragments. Therefore, the measured yields used to extract the nuclear temperature are different from the primary distributions at the freeze-out stage. This question was studied on a theoretical basis by several authors, see e.g. [28–30, 69].

Tsang et al. argued that the fluctuations observed in the value of the nuclear temperature applying different double-isotopic-ratio thermometers appear to originate from structure effects in the secondary-decay process and that each isotope ratio shows a characteristic behavior independently of the reaction [30]. Calculations performed by Xi et al. [69] indicated that due to strong feeding effects, the double-isotopic-ratio method is strongly influenced by secondary decays at temperatures above 6 MeV. Raduta and Raduta [29] have applied the sharp microcanonical multifragmentation model [56] with inclusion of secondary decay in order to evaluate the caloric curve from different isotopic thermometers for primary decay and asymptotic stages. In both stages, a dispersive character of the isotopic caloric curve increasing with the increase of the excitation energy was evidenced. The authors proposed a procedure to calibrate the isotopic thermometers on the microcanonical predictions independently of the source size and excitation energy [29].

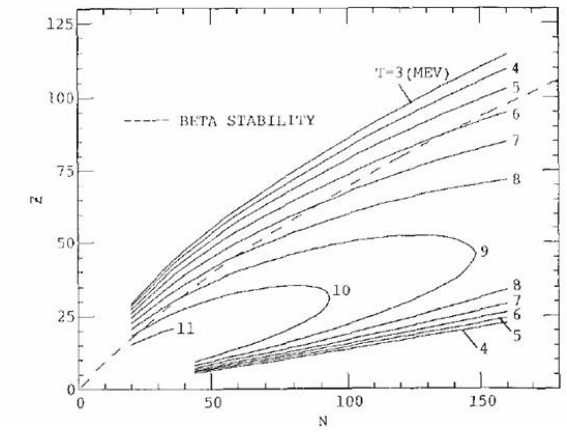


**Fig. 1.** Limiting temperatures predicted by Besprosvany and Levit [86].

A complex structure in the residue yields was recently evidenced in the fragmentation reaction $^{238}$U+Ti at 1 $A$ GeV [59]. From the light fragmentation residues, fully resolved in $A$ and $Z$, an important even-odd staggering in the yields was observed. Using the statistical model of nuclear reactions, it was shown in ref. [59] that for all classes of nuclei except for $N = Z$ nuclei structural effects in nuclear binding and in the level density are responsible for the observed staggering. The chain of $N = Z$ nuclei appears as a special class of nuclei with increased enhancement in the production of even-even nuclei compared to other chains with $N - Z$ =even, and possible origins like the Wigner energy, alpha clustering, and neutron-proton pairing were discussed [59]. Therefore, when correcting for secondary decay, complex structure, as extremely strong even-odd staggering in $N = Z$ nuclei, must be considered.

## 4 Thermometer Results

### 4.1 Nuclear Caloric Curves

As indicated in a number of previous reviews, measurements of nuclear temperatures, which have long been employed to explore excited nuclei, can also provide important information on the Van der Waals-like nuclear equation of state and the postulated liquid-gas phase transition [3,28,70–73]. A large number of theoretical calculations have explored the nuclear equation of state and reported values for the critical temperature, $T_C$, of semi-infinite nuclear matter (nuclear matter with a surface). References [74–84] constitute a representative sampling of these calculations. The different nuclear interactions employed in the calculations lead to large differences in the critical temperatures derived from these interactions. Values from 13 to 24 MeV are reported in the cited references. For finite nuclei, early theoretical work by Bonche and collaborators explored the thermal properties and stability of highly excited nuclei by employing a temperature dependent Hartree-Fock model with Skyrme interactions [8,85, 86]. This work and later work with other models [87–92] predict the existence of "limiting temperatures". The temperatures at which the expanded nucleus reaches the limit of equilibrium phase coexistence between liquid and vapor were designated "Coulomb instability" temperatures [8,85].

In extensions of the work of references [85] and [8], Besprosvany and Levit mapped the limiting temperature surface as a function of $N$ and $Z$ [86]. The limiting temperatures that they calculated are shown in Fig. 1. They are well below the critical temperature of nuclear matter. This reflects size effects, Coulomb effects and isospin asymmetry effects for the finite nuclei studied. It is important to note that such predictions are sensitive to both the chosen nuclear interaction and to the assumed temperature dependence of the surface energy [93]. One important goal of experimental measurements of temperatures of excited nuclei has been to derive information on $T_C$.

Employing a variety of Skyrme interactions Song and Su derived a mass dependent scaling of the correlation of

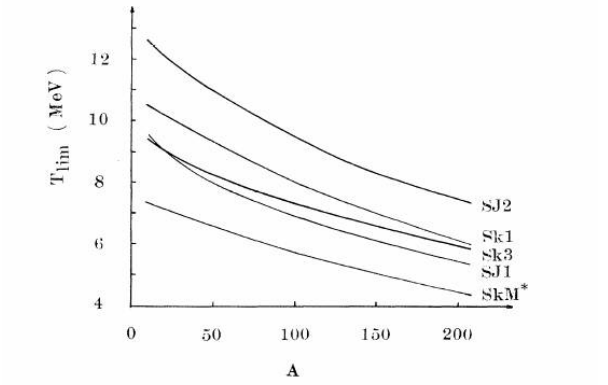


**Fig. 2.** Mass dependence of limiting temperatures for various Skyrme interactions [87].

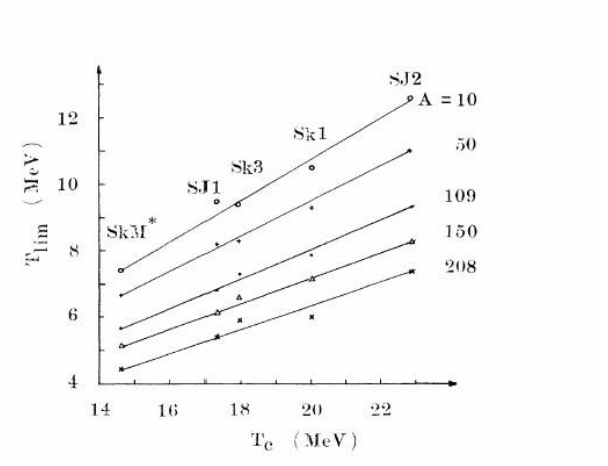


**Fig. 3.** Correlation between limiting temperature and $T_C$ for nuclear matter [87].

limiting temperatures with the critical temperature of nuclear matter [87]. Their results are shown in Figs. 2 and 3. A similar scaling exists when other model interactions are employed [87–90]. The limiting temperatures are found to be quite sensitive to $T_C$ and rather insensitive to the nuclear incompressibility, $K_{inc}$. These results, together with gathering experimental evidence of multi fragment disassembly modes at higher excitation energies, spurred the development of both statistical [4,5,94–96] and dynamic [97–104] models capable of exploring the multifragmentation process in much greater detail. Such models have made much more detailed predictions on the nature of multifragmentation processes and the excitation energy dependence of the temperature, i.e., the nuclear caloric curve.

In statistical models of multifragmentation, increasing excitation energies lead to the onset of a plateau in the temperature. This plateau occurs at a "cracking energy" which may be associated with the Coulomb instability and leads to multiple fragment production [5,94,95].

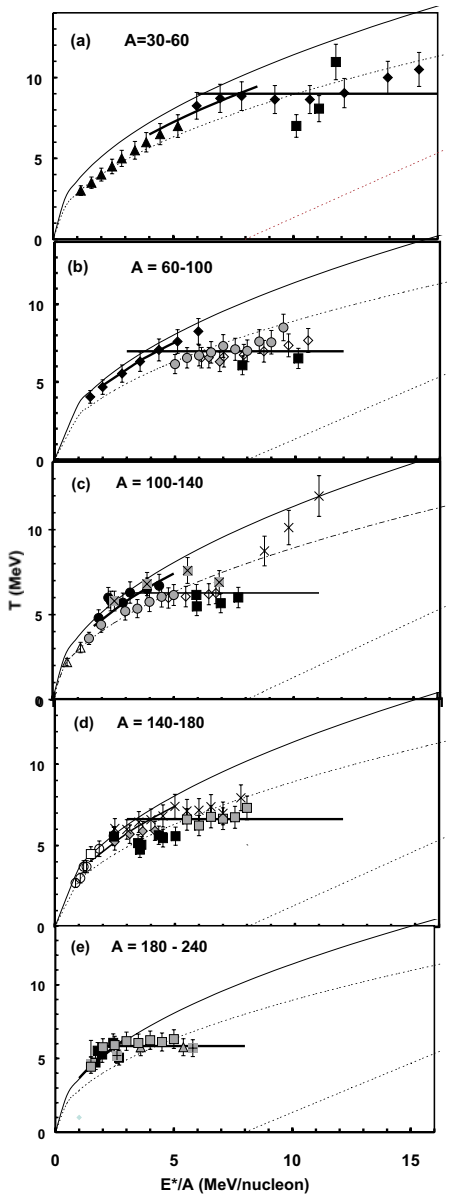


**Fig. 4.** Caloric curves for five selected regions of mass. See reference [121].

Such plateaus are also observed within the framework of classical molecular dynamics calculations [104–106] and quantum molecular dynamics calculations [107,108].

Concurrently with these theoretical studies, many experimental investigations have resulted in the construction of caloric curves [14,109–120]. In reference [121], a number of experimental caloric curves derived from charged particle observables were compared. The nature of the experimental collision dynamics encountered in the caloric curve measurements is generally such that the masses of the excited nuclei that are produced in these experiments vary as

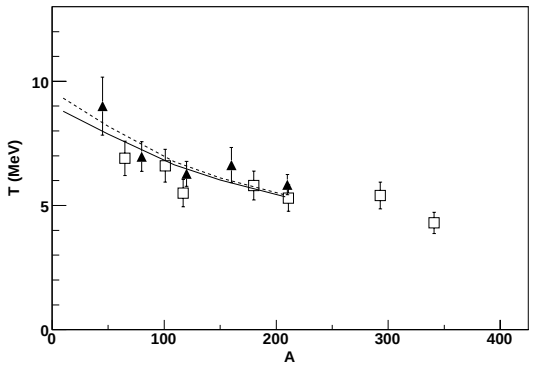


**Fig. 5.** Limiting values of temperature vs mass. Temperatures derived from double isotope ratio measurements are indicated by solid diamonds. Temperatures derived from thermal Bremsstrahlung measurements are indicated by open squares. The lines represent the calculated limiting temperatures from references [90] (dashed line) and [82] (solid line).

the excitation energy varies. Although data from different experiments exhibit significant fluctuations, caloric curves may be constructed for different mass regions selected from the available data. Such curves, presented in figure 4, are qualitatively similar and flatten into broad plateaus at higher excitation energies. Similar behavior is seen in a caloric curve derived using a very different technique, observation of "second chance" Bremsstrahlung gamma-ray emission for a series of reactions which span a wide range of mass [24,25,122].

Parameterized in terms of an inverse Fermi gas level density parameter, $k = T^2/(E_x/A)$, the data indicate that $k$ initially increases from $k \sim 8$ to $k \sim 13$ as the excitation increases. Such behavior has been explained in models which take into account the change in effective nucleon mass with excitation energy [123–127]. Beyond excitation energies corresponding to the onset of the plateau, the derived values of $k$ become progressively smaller reflecting the limiting temperature behavior seen in figure 4. An analysis of this trend, carried out assuming a nondissipative uniform Fermi gas model, indicates a rapidly increasing expansion of the nuclei with increasing excitation energy above the excitation energy where the limiting temperatures are first reached [128]. Further evidence for this expansion is found in significant barrier lowering for ejected clusters [21,129,130] as well as in coalescence radius determinations [131]. Recent papers modeling the caloric curves assuming an expanding mononucleus are in generally good agreement with the experimental data [126,127]. Nevertheless, the effect of clustering on the level density of the system needs to be better understood. In models that include clusterization, the possible existence of negative heat capacities near the onset of the plateau has been extensively discussed [5,94,132–134] and some experimental evidences for observations of such negative heat capacities have been presented [135–137]. These interpretations have been subjected to some criticism, however [138,139]. It appears that, at present, the evidence for negative heat capacities is much more secure in analogous measurements of caloric curves for atomic clusters [140,141].

Although figure 4 shows that there is a considerable spread in limiting temperature data from different measurements, the average temperatures in the plateau regions for each mass window have been employed to study the mass dependence of limiting temperatures. The limiting temperatures characterizing these plateaus decrease with increasing nuclear mass (see fig. 5).

Both, the flattening of the caloric curve and the decrease of limiting temperature with increasing mass, are in agreement with a large number of theoretical calculations. Employing Fisher scaling analysis, Elliott et al. [142] concluded that the critical temperature for a nucleus with $A \sim 168$ at $E_x/A = 3.8$ MeV is 6.7 MeV. This temperature is in good agreement with the limiting temperature deduced from the caloric curve. It appears that the point identified as the critical point by the droplet analysis is the point of initial flattening of the caloric curve.

### 4.2 Caloric Curves and the Nuclear Equation of State

In reference [143], the mean variation of $T_{lim}/T_C$ with $A$, determined from commonly used microscopic theoretical calculations has been used, together with the five experimental limiting temperatures reported in reference [121], to extract a critical temperature of nuclear matter of $16.6 \pm 0.86$ MeV. Using a relationship between parameters used to describe nuclear matter suggested by Kapusta [144] and Lattimer and Swesty [145] both the incompressibility and the effective mass can be derived. The compressibility modulus for moderately excited nuclei, determined from the critical temperature in this manner is consistent with that determined from measurements of the nuclear Giant Monopole Resonance [146]. In attempts to derive the nuclear matter coexistence curve from Fisher scaling analysis nuclear matter critical temperatures of 10 to 14 MeV have been obtained [147]. These values are surprisingly close to the values derived for the finite systems studied [148]. Here, again, the temperature dependence of the surface energy plays an important role in the extrapolation to nuclear matter.

### 4.3 Temperature Evolution

Both dynamic and thermodynamic considerations lead us to expect significant temperature changes as the reactions progress. Thus, probing the thermal evolution of the system can provide considerably more information on the history and degree of equilibration of the collisionally heated systems. In some recent measurements, the kinetic energy variation of emitted light clusters has been employed as a clock to explore the time evolution of the temperature for thermalizing composite systems in the reactions of $26A$, $35A$ and $47A$ MeV $^{64}$Zn with $^{58}$Ni, $^{92}$Mo and $^{197}$Au [149].

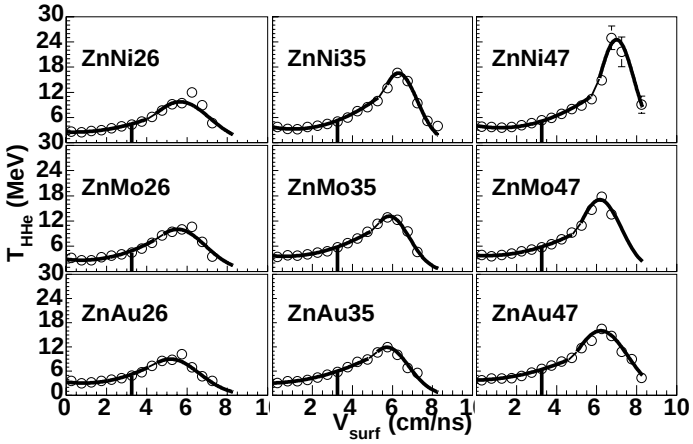


**Fig. 6.** $T_{HHe}$ vs surface velocity. See text. Horizontal bars are at 3-3.5 cm/ns corresponding to entry into the evaporation phase of the reaction. Solid lines indicate fits to data.

Figure 6 presents experimental results for the double isotope ratio temperatures as a function of velocity in the nucleon center of mass frame.

For the earliest stages of the collision, transport model calculations demonstrate a strong correlation of decreasing surface velocity with increasing time [149]. For each system investigated the double isotope ratio temperature curve exhibits a high maximum apparent temperature, in the range of 10-25 MeV, at high ejectile velocity. These maximum values increase with increasing projectile energy and decrease with increasing target mass and are much higher than the limiting temperatures determined from caloric curve measurements in similar reactions.

In each case, the temperature then decreases monotonically as the velocity decreases below the velocity at which the maximum is seen. The maxima in the temperature curves appear to signal the achievement of chemical equilibrium (a pre-requisite for employment of double isotope temperatures) at least on a local basis. They are quite comparable to those reported for QMD transport model calculations of the maximum and average temperatures and densities achieved in symmetric or near symmetric heavy ion collisions [150]. Those results strongly suggest the presence of an initial hot, locally equilibrated, participant zone surrounded by colder spectator matter. A similar picture is obtained in the AMD-V calculations of reference [151]. For each different target, the subsequent cooling as the ejectile velocity decreases is quite similar. Temperatures comparable to those of limiting temperature systematics are reached at times when AMD-V transport model calculations predict entry into the final evaporative or fragmentation stage of de-excitation of the hot composite systems. Calibration of the time-scales using AMD-V calculations indicate that this occurs at times ranging from ∼135 fm/c for the Ni target to ∼165 fm/c for Au [149].

## 5 Conclusions

From all what was said, it is clear that it is not straightforward to determine the thermodynamical temperature $T$ ($1/T = \partial S/\partial E$) of a nuclear system. Important theoretical progress in understanding the conceptual differences in the apparent temperature values obtained from the different experimental methods has been made in last ten years. Also on the experimental side, efforts have been made in order to obtain more information on the influence of the reaction dynamics on the apparent temperature values.

An enormous complexity of effects involved in the interpretation of apparent-temperature measurements has been evidenced. Understanding of these effects helped in approaching the results obtained using different thermometer methods. The question is whether we still have more complexity to expect. Le Fèvre et al. [55] have shown that apparent temperatures, even if uncertain in absolute value, seem to be surprisingly robust in showing signatures of phase transitions. In other words, caloric curves obtained using some of the above mentioned thermometer methods can still carry the signal of the phase transition in a system with conserved energy.

On the other hand, for the systems already studied, the differences in the entrance channel isospins and in the first stage dynamics lead to some variation of the isospin of the fragmenting nuclei. However, the systematic uncertainties in the present measurements are such that sensitivity to this variable is not obvious. In the future, extension of caloric curve measurements to nuclei far from stability should be very instructive. With the proposed radioactive beam facilities it will be possible to employ caloric curve measurements to determine the critical parameters for quite asymmetric nuclei. In the future, determination of the nuclear level densities, of the limiting temperatures and of critical temperatures for asymmetric nuclear matter will play a significant role in providing a means to establish the isospin dependence of the nuclear equation of state and the nature of the phase transition in asymmetric nuclear matter.

## References


1. H.A. Bethe, Rev. Mod. Phys. **9** (1937) 69
2. V.F. Weisskopf, Phys. Rev. **52** (1937) 295
3. E. Suraud, Ch. Grégoire and B. Tamain, Prog. Part. Nucl. Phys. **23** (1989) 357
4. D.H.E. Gross, Rep. Prog. Phys. **53** (1990) 605
5. J.P. Bondorf et al., Phys. Rep. **257** (1995) 133
6. D.J. Morrissey, Annu. Rev. Nucl. Part. Sci. **44** (1994) 27
7. D.H.E. Gross, Entropy **6** (2004) 158
8. S. Levit and P. Bonche, Nucl. Phys. A **437** (1985) 426
9. S. Albergo et al., Nuovo Cimento A **89** (1985) 1
10. J. Pochodzalla et al., Phys. Rev. Lett. **75** (1995) 1040
11. D.J. Morrissey et al., Phys. Lett. B **148** (1984) 423
12. D.J. Morrissey et al., Phys. Rev. C **32** (1985) 877
13. J. Pochodzalla et al., Phys. Rev. Lett. **55** (1985) 177
14. J. Pochodzalla et al., Phys. Rev. C **35** (1987) 35
15. G.J. Kunde et al., Phys. Lett. B **272** (1991) 202
16. V. Serfling et al., Phys. Rev. Lett. **80** (1998) 3928
17. M. Veselsky et al., Phys. Lett. B **497** (2001) 1
18. M. Veselsky et al., Phys. Part. Nucl. **36** (2005) 213
19. G.D. Westfall, Phys. Lett. B **116** (1982) 118
20. B.V. Jacak et al., Phys. Rev. Lett. **51** (1983) 1846
21. G.D. Westfall et al., Phys. Rev. C **17** (1978) 1368
22. T. Odeh et al., Phys. Rev. Lett. **84** (2000) 4557
23. J. Gosset et al., Phys. Rev. C **16** (1977) 629
24. D.G. d'Enterria et al., Phys. Lett. B **538** (2002) 27
25. R. Ortega et al., Nucl. Phys. A **734** (2004) 541
26. K.-H. Schmidt et al., Phys. Lett. B **300** (1993) 313
27. K.-H. Schmidt et al., Nucl. Phys. A **710** (2002) 157
28. S. Shlomo et al., Rep. Prog. Phys. **68** (2005) 1
29. Al.H. Raduta et al., Nucl. Phys. A **671** (2000) 609
30. M.B. Tsang et al., Phys. Rev. Lett. **78** (1997) 3836
31. D.H. Boal, Phys. Rev. C **30** (1984) 749
32. A.S. Goldhaber, Phys. Rev. C **17** (1978) 2243
33. W.A. Friedman and W.G. Lynch, Phys. Rev. C **28** (1983) 16
34. I. Dostrowsky, P. Robinowitz and P. Bivins, Phys. Rev. **111** (1958) 1659
35. R. Pühlhofer, Nucl. Phys. A **280** (1977) 267
36. A. Gavron, Phys. Rev. C **21** (1980) 230
37. M. Blann, Phys. Rev. C **23** (1981) 205
38. R.J. Charity et al., Nucl. Phys. A **483** (1988) 371
39. S. Ban-Hao and D. H. E. Gross, Nucl. Phys. A **437** (1985) 643
40. A.S. Goldhaber, Phys. Lett. B **53** (1974) 306
41. D.J. Fields et al., Phys. Rev. C **30** (1984) 1912
42. H. Stöcker et al., Z. Phys. A **303** (1981) 259
43. W.A. Friedman and W.G. Lynch, Phys. Rev. C **28** (1983) 950
44. W.A. Friedman, Phys. Rev. C **37** (1988) 976
45. C.B. Chitwood et al., Phys. Rev. C **34** (1986) 858
46. P.J. Siemens and J.O. Rasmussen, Phys. Rev. Lett. **42** (1979) 880
47. W.A. Friedmann, Phys. Rev. C **42** (1990) 667
48. N. Marie et al., Phys. Rev. C **58** (1998) 256
49. S. Hudan et al., Phys. Rev. C **67** (2003) 064613
50. H. Müller and B.D. Serot, Phys. Rev. C **52** (1995) 2072
51. V. Baran et al., Nucl. Phys. A **703** (2002) 603
52. D. Henzlova, Ph.D. thesis, University of Prague, March 2006
53. L. Shi and P. Danielewicz, Phys. Rev. C **68** (2003) 064604
54. H. Xi et al., Phys. Lett. B **431** (1998) 8
55. A. Le Fèvre et al., Nucl. Phys. A **657** (1999) 446
56. Al.H. Raduta et al., Phys. Rev. C **59** (1999) R1855
57. V.E. Viola et al., Phys. Rev. C **59** (1999) 2660
58. S. Hudan et al., Phys. Rev. C **71** (2005) 054604
59. M.V. Ricciardi et al., Nucl. Phys. A **733** (2004) 299
60. S.K. Samaddar et al., Phys. Rev. C **71** (2005) 011601
61. D.H.E. Gross, Phys. Rep. **279** (1997) 119
62. J.A. Hauger et al., Phys. Rev. Lett. **77** (1996) 235
63. Y.G. Ma et al., Phys. Lett. B **390** (1997) 41
64. T.X. Liu et al., Phys. Rev. C **69** (2004) 014603
65. M. Colonna et al., Phys. Rev. Lett. **88** (2002) 122701
66. T. Sill et al., Phys. Rev. C **69** (2004) 014602
67. E. Vient et al., Nucl. Phys. A **700** (2002) 555
68. S. Pal et al., Nucl. Phys. A **586** (1995) 466
69. H. Xi et al., Phys. Rev. C **59** (1999) 15667
70. B. Tamain and D. Durand, University of Caen Report LPCC 96-16 (1996)
71. P. Chomaz, *Proc. of the Int. Nucl. Phys. Conf. INPC2001*, Berkeley CA, USA, 2001, ed. by E. Norman, L. Schroeder, G. Wozniak, AIP Conference Proceedings (Melville, New York 2002), p. 167
72. A. Bonasera et al., Riv. Del Nuovo Cimento **23** (2) (2000) 1-101
73. S. Das Gupta et al., nucl-th/0009033
74. J.P. Blaizot, Phys. Rep. **64** (1980) 171
75. H. Jaqaman et al., Phys. Rev. C **27** (1983) 2782; ibid **29** (1984) 2067
76. W.D. Myers and W.J. Swiatecki, Phys. Rev. C **57** (1998) 3020
77. J. Zimanyi and S.A. Moszkowski, Phys. Rev. C **42** (1990) 1416
78. P.G. Reinhard et al., Z. Phys. A **323** (1986) 13
79. J.P. Blaizot et al., Nucl. Phys. A **591** (1995) 435
80. R.J. Furnstahl et al., Nucl. Phys. A **615** (1997) 441
81. G. Lalazissis et al., Phys. Rev. C **55** (1997) 540
82. M. Malheiro et al., Phys. Rev. C **58** (1998) 426
83. E. Chabanat et al., Nucl. Phys. A **627** (1997) 710
84. M. Farine et al., Nucl. Phys. A **615** (1997) 135
85. P. Bonche et al., Nucl. Phys. A **427** (1984) 278
86. J. Besprosvany and S. Levit, Phys. Lett. B **217** (1989) 1
87. H.Q. Song and R.K. Su, Phys. Rev. C **44** (1991) 2505
88. H.Q. Song et al., Phys. Rev. C **47** (1993) 2001; ibid **49** (1994) 2924
89. Y. Zhang et al., Phys. Rev. C **54** (1996) 1137
90. M. Baldo and L. S. Ferreira, Phys. Rev. C **59** (1999) 682
91. J.N. De et al., Phys. Rev. C **55** (1997) R1641
92. P. Wang et al., Nucl. Phys. A **748** (2005) 226
93. A.L. Goodman et al., Phys. Rev. C **30** (1984) 851
94. W.A. Friedman, Phys. Rev. Lett. **60** (1988) 2125
95. J. Aichelin et al., Phys. Rev. C **37** (1988) 2451
96. F. Gulminelli and D. Durand, Nucl. Phys. A **615** (1997) 117
97. J. Schnack and H. Feldmeier, Phys. Lett. B **409** (1997) 6
98. C. Fuchs et al., Nucl. Phys. A **626** (1997) 987
99. H. Kruse et al., Phys. Rev. C **31** (1985) 170
100. H. Horiuchi, Nucl. Phys. A **583** (1995) 297c
101. A. Ono, Phys. Rev. C **59** (1999) 853
102. P. Chomaz et al., Phys. Rev. Lett. **73** (1994) 3512
103. W. Nörenberg et al., Euro. Phys. J. A **9** (2000) 327; ibid **14** (2002) 43
104. A. Chernomoretz et al., Phys. Rev. C **64** (2001) 044605
105. A. Strachan and C. O. Dorso, Phys. Rev. C **58** (1998) 632

106. M.J. Ison et al., Physica A **341** (2004) 389
107. Y. Sugawa and H. Horiuchi, Prog. Theor. Phys. **105** (2001) 131
108. T. Furuta and A. Ono, Prog. Theor. Phys. Suppl. **156** (2004) 147
109. K. Hagel et al., Nucl. Phys. A **486** (1988) 429
110. R. Wada et al., Phys. Rev. C **39** (1989) 497
111. D. Cussol et al., Nucl. Phys. A **561** (1993) 298
112. M. Gonin et al., Phys. Rev. C **42** (1990) 2125
113. T. Odeh, GSI Report Diss. **99-15**, August 1999, and references therein
114. J.A. Hauger et al., Phys. Rev. C **62** (2000) 024616
115. R. Wada et al., Phys. Lett. B **423** (1998) 21
116. K.B. Morley et al., Phys. Rev. C **54** (1996) 737; ibid, **54** (1996) 749
117. J. Cibor et al., Phys. Lett. B **473** (2000) 29
118. K. Hagel et al., Phys. Rev. C **62** (2000) 034607-1
119. A. Ruangma et al., Phys. Rev. C **66** (2002) 044603
120. B. Borderie, *Proc. of the Conference: Bologna 2000*, Bologna, Italy, 2000, ed. by G.C. Bonsignori et al., World Scientific (Singapore 2001), Vol. 1 Nucleus-Nucleus Collisions, p.187, preprint nucl-ex/0102016
121. J.B. Natowitz et al., Phys.Rev. C **65** (2002) 034618
122. D.G. d'Enterria et al., Phys. Rev. Lett. **87** (2002) 22701
123. R. Hasse and P. Schuck, Phys. Lett. B **179** (1986) 313
124. S. Shlomo and J.B. Natowitz, Phys. Lett. B **252** (1990) 187
125. S. Shlomo and J.B. Natowitz, Phys. Rev. C **44** (1991) 2878
126. L.G. Sobotka et al., Phys. Rev. Lett. **93** (2004) 132702
127. J.N. De et al., Phys. Lett. B **638** (2006) 160
128. J.B. Natowitz et al., Phys.Rev. C **66** (2002) 031601
129. A.S. Hirsch et al., Phys. Rev. C **29** (1984) 508
130. V.E. Viola et al., Phys. Rev. Lett. **93** (2004) 132701
131. J. Cibor et al., In "Isospin Physics in Heavy-Ion Collisions at Intermediate Energies", Eds. Bao-An Li and W.U. Schroeder, NOVA Science Publishers, Inc. (New York), (2001)
132. D.H.E. Gross et al., Ann. Phys. **5** (1996) 446
133. P. Chomaz et al., Phys. Rev. Lett. **85** (2000) 3587
134. P. Chomaz and F. Gulminelli, Phys. Lett. B **447** (1999) 221
135. D.H.E. Gross and J.F. Kenney, J. Chem. Phys. **122** (2005) 224111
136. A. Chbihi et al., Eur. Phys. J. A **5** (1999) 251
137. M. D'Agostino et al., Nucl. Phys. A **650** (1999) 329
138. W. Thirring et al., Phys. Rev. Lett. **91** (2003) 130601
139. X. Campi et al., Phys. Rev. C **71** (2005) 041601
140. M. Schmidt et al., Phys. Rev. Lett. **87** (2001) 203402
141. D.H.E. Gross and P.A. Hervieux , Zeit. Fuer Phys. D **35** (1995) 27
142. J.B. Elliott et al., Phys. Rev. Lett. **88** (2002) 042701
143. J.B. Natowitz et al., Phys. Rev. Lett. **89** (2002) 212701
144. J. Kapusta, Phys. Rev. C **29** (1984) 1735
145. J.M. Lattimer and F.D. Swesty, Nucl. Phys. A **535** (1991) 331
146. D.H. Youngblood et al., Phys. Rev. Lett. **82** (1999) 691
147. L.G. Moretto et al., Phys. Rev. C **72** (2005) 064605
148. J.B. Elliott et al., Phys. Rev. C **67** (2003) 024609
149. J. Wang et al., Phys. Rev. C **72** (2005) 024603
150. A.D. Sood and R.K. Puri, Phys. Rev. C **70** (2004) 034611
151. R. Wada et al., Phys.Rev. C **69** (2004) 044610